*I. Arasaratnam and K. P. Bharani Chandra*

# *Cubature Information Filters: Theory and Applications to Multisensor Fusion*

# *Contents*

# List of Figures

# 1

# *Cubature Information Filters: Theory and Applications to Multisensor Fusion*

**CONTENTS**



## 1.1 Introduction

Sensor fusion is generally defined as the use of techniques that combine data from multiple sensors such that the resulting information is more accurate and more reliable than that from a single sensor. Sensor fusion techniques are widely used in many applications such as mobile robot navigation, surveillance, air-traffic control and intelligent vehicle operations. For multiple sensor fusion in a linear Gaussian environment, the information filter, which can be considered as the dual of the Kalman filter, has been a viable solution [3,4,10]. Although the Kalman filter and the information filter are algebraically equivalent, the Kalman filter propagates a state vector and its error covariance whereas the information filter uses an information vector and an information matrix. This difference makes the information filter to be superior to the Kalman filter in fusion problems because computations are straight-forward and simple. Moreover, no prior information about the system state is required.

For nonlinear fusion problems however, it is difficult to obtain an optimal solution. In the past, researchers have closely followed the linear fusion theory

to obtain a suboptimal solution for nonlinear fusion problems. Recently, Vercauteren *et al.* derived the sigma-point information filter using the statistical linear regression theory and the unscented transformation [9] whereas Kim *et al.* derived a similar set of steps using a minimum mean squared-error criterion [7]. When we are confronted with an issue of striking the appropriate balance or trade-off between accuracy and computational complexity, the cubature Kalman filter (CKF) is considered to be the logical choice [2]. The CKF is a more accurate and stable estimation algorithm than the unscented/sigma-point filter. However, due to the fact that the sigma-point filter and the CKF share a number common characteristics, the derivation of the Cubature Information Filter (CIF) is straightforward and hence trivial. In this chapter, we focus on to derive the square-root version of the CIF for improved numerical stability. Unlike the CIF, the SCIF avoids numerically sensitive matrix operations such as matrix square-rooting and inversion.

The rest of the chapter is organized as follows: The next section reviews information filtering in general. We then derive the SCIF using the linear fusion theory and matrix algebra. In order to validate the formulation and reliability of the SCIF, it is applied to couple of multisensor fusion problems. The chapter concludes with some remarks.

## 1.2 Information Filtering: A Brief Review

The information filter is a modified version of the Kalman filter– The state estimates and their corresponding covariances in the Kalman filter are replaced by the information vectors and information matrices (inverse covariances), respectively, in the information filter. The updated covariance and the updated state take the information form, as shown by

$$\mathbf{Y}_{k|k} = \mathbf{P}_{k|k}^{-1} \tag{1.1}$$

$$\hat{\mathbf{y}}_{k|k} = \mathbf{P}_{k|k}^{-1}\hat{\mathbf{x}}_{k|k}. \tag{1.2}$$

Similarly, the predicted covariance and the predicted state have equivalent information forms:

$$\mathbf{Y}_{k+1|k} = \mathbf{P}_{k+1|k}^{-1} \tag{1.3}$$

$$\hat{\mathbf{y}}_{k+1|k} = \mathbf{P}_{k+1|k}^{-1}\hat{\mathbf{x}}_{k+1|k} \tag{1.4}$$

At the heart of any one of information filters lies the information update, which now becomes a trivial sum.

$$\mathbf{Y}_{k+1|k+1} = \mathbf{Y}_{k+1|k} + \mathcal{I}_{k+1} \tag{1.5}$$

$$\hat{\mathbf{y}}_{k+1|k+1} = \hat{\mathbf{y}}_{k+1|k} + \mathbf{i}_{k+1} \tag{1.6}$$

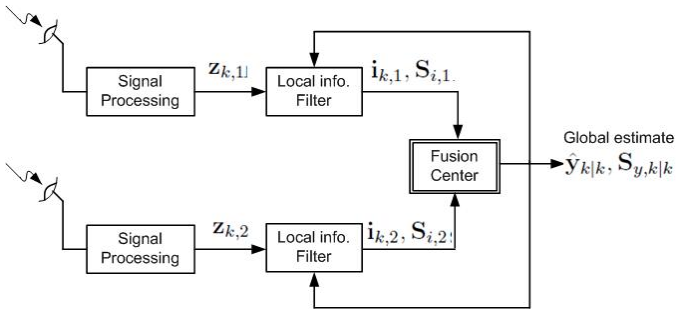


**FIGURE 1.1**
Information flow in a distributed sensor configuration with feedback

Here, the information contribution matrix and the information contribution vector are defined as follows, respectively [7, 9]:

$$\mathcal{I}_{k+1} = \left(\mathbf{Y}_{k+1|k}\mathbf{P}_{xz,k+1|k}\right)\mathbf{R}_{k+1}^{-1}\left(\mathbf{Y}_{k+1|k}\mathbf{P}_{xz,k+1|k}\right)^{\mathrm{T}} \quad (1.7)$$

$$\mathbf{i}_{k+1} = \left(\mathbf{Y}_{k+1|k}\mathbf{P}_{xz,k|k}\right)\mathbf{R}_{k+1}^{-1}\left(\mathbf{z}_{k+1} - \hat{\mathbf{z}}_{k+1|k} + \mathbf{P}_{xz,k+1|k}^{\mathrm{T}}\hat{\mathbf{y}}_{k+1|k}\right) \quad (1.8)$$

### 1.2.1 Information Fusion

In the sensor fusion literature, there are a number of sensor networks with their own virtues and limitations [4]. In this chapter, we specifically consider a distributed configuration with feedback [10]. As shown in Fig. 1.1, in this network, each local sensor has its own information processor. The locally processed results are then transmitted to the fusion center for computing a global estimate. The global estimate is broadcast so that all the local sensors utilize the global estimate for the purpose of processing the next measurement. The advantage of using the information filters within the local sensors is that the global estimate in the fusion center can be computed from $n_s$ sensor measurements at each time step by simply summing the local information vectors and matrices:

$$\hat{\mathbf{y}}_{k|k} = \hat{\mathbf{y}}_{k|k-1} + \sum_{s=1}^{n_s}\mathbf{i}_{k,s} \quad (1.9)$$

$$\mathbf{Y}_{k|k} = \mathbf{Y}_{k|k-1} + \sum_{s=1}^{n_s}\mathcal{I}_{k,s} \quad (1.10)$$

Note that the computations outlined in this section hold under the following assumptions: (i). The tracking problem at hand is described by a linear Gaussian system. (ii). The sensor measurements are uncorrelated to each other. (iii). There is no measurement origin of ambiguity. (iv). The sensors are synchronized (v). There is no receipt of out-of sequence measurements (vi). There

is no communication loss among sensors. When one or more of these conditions are violated, various techniques have been proposed to get around them in the literature [4].

## 1.3 Square-root Cubature Information Filtering

In each recursion cycle, it is important that we preserve the two properties of an information matrix, namely, its positive definitiveness and symmetry. Unfortunately, when the CIF is committed to an embedded system with limited word-length, numerical errors may lead to a loss of these properties. The accumulation of numerical errors may cause the information filter to diverge or otherwise crash. The CIF involves numerically sensitive operations such as matrix square-rooting and matrix inversion, which may combine to destroy the fundamental properties of an information matrix. The logical procedure to preserve both properties of the information matrix and to improve the numerical stability is to design a square-root version of the CIF. Although the square-root cubature information filter (SCIF) is reformulated to propagate the square-roots of the information matrices, both the CIF and the SCIF are algebraically equivalent to other.

Before deriving the SCIF, for convenience, we introduce the following notations:

- We denote a general triangularization algorithm (e.g., QR decomposition) as $\mathbf{S} = \mathbf{Tria}(\mathbf{A})$, where $\mathbf{S}$ is a lower triangular matrix. The matrices $\mathbf{A}$ and $\mathbf{S}$ are related to each other as follows: Let $\mathbf{R}$ be an upper triangular matrix obtained from the QR decomposition on $\mathbf{A}^T$; then $\mathbf{S} = \mathbf{R}^T$.
- We use $\mathbf{S}_{Q,k}$ and $\mathbf{S}_{R,k}$ to denote the square-roots of $\mathbf{Q}_k$ and $\mathbf{R}_k$, respectively. That is, $\mathbf{Q}_k = \mathbf{S}_{Q,k}\mathbf{S}_{Q,k}^{\mathrm{T}}$ and $\mathbf{R}_k = \mathbf{S}_{R,k}\mathbf{S}_{R,k}^{\mathrm{T}}$.

Because many of the SCIF computations can be easily borrowed from the SCKF [1], we only derive the steps that require explicit treatments in the sequel. Like the SCKF, the SCIF also includes two steps, namely, the time update and the measurement update.

### 1.3.1 Time Update

Let $\mathbf{Y}_{k|k}$ be

$$\mathbf{Y}_{k|k} = \mathbf{S}_{y,k|k}\mathbf{S}_{y,k|k}^{\mathrm{T}} \tag{1.11}$$

and $\mathbf{Y}_{k+1|k}$ be

$$\mathbf{Y}_{k+1|k} = \mathbf{S}_{y,k+1|k}\mathbf{S}_{y,k+1|k}^{\mathrm{T}}. \tag{1.12}$$

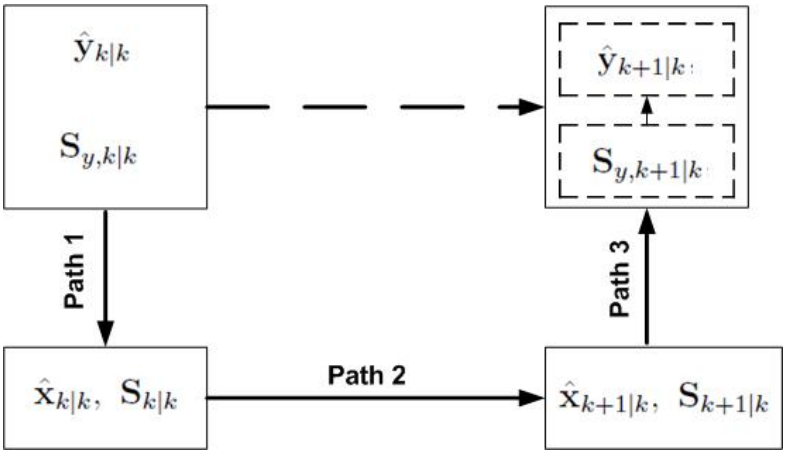


**FIGURE 1.2**
Time update of the SCIF

As depicted in Fig. 1.2, the time update of the SCIF connects $(\hat{\mathbf{y}}_{k|k}, \mathbf{S}_{y,k|k})$ to $(\hat{\mathbf{y}}_{k+1|k}, \mathbf{S}_{y,k+1|k})$ via three paths. Let us first consider how to derive Path 1, in which the information space is projected onto the state space. Taking inverse on both sides of (1.1), we get

$$\mathbf{P}_{k|k} = \mathbf{Y}_{k|k}^{-1}. \tag{1.13}$$

Substituting the square-root factors on both side of (1.13) yields

$$\begin{aligned} \mathbf{S}_{k|k}\mathbf{S}_{k|k}^{\mathrm{T}} &= \left(\mathbf{S}_{y,k|k}\mathbf{S}_{y,k|k}^{\mathrm{T}}\right)^{-1} \\ &= \mathbf{S}_{y,k|k}^{-\mathrm{T}}\mathbf{S}_{y,k|k}^{-1} \end{aligned} \tag{1.14}$$

We may therefore write the square-root of the error covariance matrix

$$\mathbf{S}_{k|k} = \mathbf{S}_{y,k|k}^{-\mathrm{T}} \tag{1.15}$$

We summarize the following important result from (1.13) and (1.15) as follows:

$$\boxed{\mathbf{P}_{k|k} = \mathbf{Y}_{k|k}^{-1}} \quad \Rightarrow \quad \boxed{\mathbf{S}_{k|k} = \mathbf{S}_{y,k|k}^{-\mathrm{T}}}. \tag{1.16}$$

Because $\mathbf{S}_{y,k|k}$ is a triangular matrix, the least-squares method can be used to avoid computing its inversion explicitly [6]. From (1.2), we write the updated state estimate

$$\begin{aligned} \hat{\mathbf{x}}_{k|k} &= \mathbf{P}_{k|k}\hat{\mathbf{y}}_{k|k} \\ &= \mathbf{S}_{k|k}\mathbf{S}_{k|k}^{\mathrm{T}}\hat{\mathbf{y}}_{k|k}, \end{aligned} \tag{1.17}$$

which completes Path 1.

As shown in Fig. 1.2, Path 3 is an inverse projection (from the state space to the information space) of Path 1. By closely following this idea and using (1.3)-(1.4), the state space quantities can be projected back onto the information space to obtain Path 3. Because Path 2 is identical to the time update of the SCKF, the reader may refer to Section VII of [1] for a detailed derivation.

### 1.3.2 Measurement Update

In the measurement update step, we will see how to fuse a new measurement with the predicted information to obtain the updated information. As depicted in Fig. 1.3, the measurement update step also includes three paths. Consider Path 1. Given $\hat{\mathbf{x}}_{k+1|k}$ and $\mathbf{S}_{k+1|k}$, the predicted measurement $\hat{\mathbf{z}}_{k+1|k}$ and the sub-matrices of the transformation matrix $\mathbf{T}$, namely, $\mathbf{T}_{11}$ and $\mathbf{T}_{21}$ can be obtained as described in Section VII of [1]. Fortunately, $\hat{\mathbf{x}}_{k+1|k}$ and $\mathbf{S}_{k+1|k}$ are available as the by-products of the time update of the SCIF, specifically, from Path 2 of the time update. For this reason, we do not describe the derivation of Path 1 in this chapter.

Let us derive Path 2 now. The end products of Path 2 are the information contribution vector ($\mathbf{i}_{k+1}$), and the square-root information contribution matrix $\left(\mathbf{S}_{i,k+1}\right)$. First, we will derive $\mathbf{S}_{i,k+1}$. By closely following (1.16), we may write the inverse of the measurement noise covariance matrix

$$\bar{\mathbf{S}}_{R,k} \quad = \quad \mathbf{S}_{R,k}^{-\mathrm{T}}. \tag{1.18}$$

Substituting (1.18) into (1.7) and rearranging the right hand side, we get

$$\mathcal{I}_{k+1} \quad = \quad \left(\mathbf{Y}_{k+1|k}\mathbf{P}_{xz,k+1|k}\bar{\mathbf{S}}_{R,k+1}\right)\left(\mathbf{Y}_{k+1|k}\mathbf{P}_{xz,k+1|k}\bar{\mathbf{S}}_{R,k+1}\right)^{\mathrm{T}} \tag{1.19}$$

Therefore, from (1.19), we may write $\mathcal{I}_{k+1}$ in a factored form:

$$\mathcal{I}_{k+1} \quad = \quad \mathbf{S}_{i,k+1}\mathbf{S}_{i,k+1}^{\mathrm{T}}, \tag{1.20}$$

where the square-root information matrix of dimension $(n \times m)$ is defined as

$$\mathbf{S}_{i,k+1} \quad = \quad \mathbf{Y}_{k+1|k}\mathbf{P}_{xz,k+1|k}\bar{\mathbf{S}}_{R,k+1} \tag{1.21}$$

$$\quad = \quad \mathbf{S}_{y,k+1|k}\mathbf{S}_{y,k+1|k}^{\mathrm{T}}\mathbf{P}_{xz,k+1|k}\bar{\mathbf{S}}_{R,k+1}. \tag{1.22}$$

Because $\mathbf{P}_{xz,k+1|k} = \mathbf{T}_{21}\mathbf{T}_{11}^{\mathrm{T}}$ (see (37) of [1]), we finally write (1.22) as

$$\boxed{\mathbf{S}_{i,k+1} = \mathbf{S}_{y,k+1|k}\mathbf{S}_{y,k+1|k}^{\mathrm{T}}\mathbf{T}_{21}\mathbf{T}_{11}^{\mathrm{T}}\bar{\mathbf{S}}_{R,k+1}} \tag{1.23}$$

Moving on to determining $\mathbf{i}_{k+1}$, we rewrite (1.4) as

$$\hat{\mathbf{y}}_{k+1|k} \quad = \quad \mathbf{Y}_{k+1|k}\hat{\mathbf{x}}_{k+1|k} \tag{1.24}$$

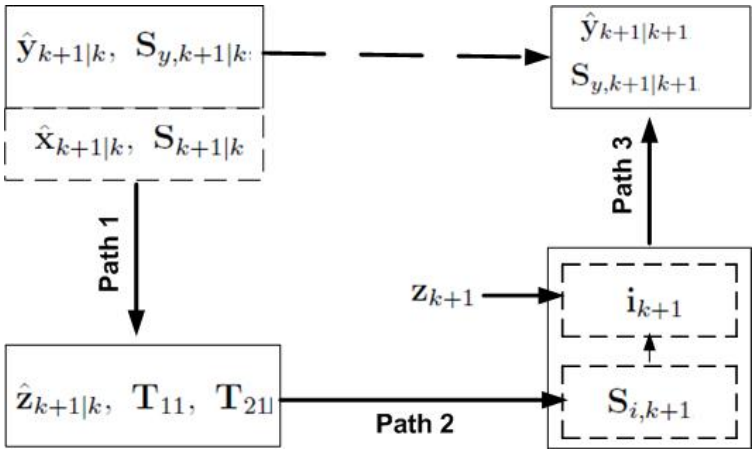


**FIGURE 1.3**
Measurement update of the SCIF

Because $\mathbf{Y}_{k+1|k}$ is a symmetric matrix, we may also write (1.24) as

$$\hat{\mathbf{y}}_{k+1|k} = \mathbf{Y}_{k+1|k}^{\mathrm{T}}\hat{\mathbf{x}}_{k+1|k} \tag{1.25}$$

Substituting (1.25) into (1.8) yields

$$\begin{aligned}\mathbf{i}_{k+1} &= \mathbf{Y}_{k+1|k}\mathbf{P}_{xz,k+1|k}\mathbf{R}_{k+1}^{-1}\big(\mathbf{z}_{k+1} - \hat{\mathbf{z}}_{k+1|k} + \\ &\quad \mathbf{P}_{xz,k+1|k}^{\mathrm{T}}\mathbf{Y}_{k+1|k}^{\mathrm{T}}\hat{\mathbf{x}}_{k+1|k}\big) \\ &= \mathbf{Y}_{k+1|k}\mathbf{P}_{xz,k+1|k}\bar{\mathbf{S}}_{R,k+1}\bar{\mathbf{S}}_{R,k+1}^{\mathrm{T}}\big(\mathbf{z}_{k+1} - \hat{\mathbf{z}}_{k+1|k} + \\ &\quad \mathbf{P}_{xz,k+1|k}^{\mathrm{T}}\mathbf{Y}_{k+1|k}^{\mathrm{T}}\hat{\mathbf{x}}_{k+1|k}\big)\end{aligned} \tag{1.26}$$

Substituting (1.21) into (1.26) and expanding the right hand side yields

$$\boxed{\mathbf{i}_{k+1} = \mathbf{S}_{i,k+1}\bar{\mathbf{S}}_{R,k+1}\big(\mathbf{z}_{k+1} - \hat{\mathbf{z}}_{k+1|k}\big) + \mathbf{S}_{i,k+1}\mathbf{S}_{i,k+1}^{\mathrm{T}}\hat{\mathbf{x}}_{k+1|k}} \tag{1.27}$$

Consider Path 3 now. The updated information vector $\hat{\mathbf{y}}_{k+1|k+1}$ can be computed by substituting (1.27) into (1.6). To obtain the updated information matrix $\mathbf{Y}_{k+1|k+1}$, we replace the right hand side of with square-roots and write

$$\begin{aligned}\mathbf{Y}_{k+1|k+1} &= \mathbf{S}_{y,k+1|k}\mathbf{S}_{y,k+1|k}^{\mathrm{T}} + \mathbf{S}_{i,k+1}\mathbf{S}_{i,k+1}^{\mathrm{T}} \\ &= [\mathbf{S}_{y,k+1|k} \quad \mathbf{S}_{i,k+1}][\mathbf{S}_{y,k+1|k} \quad \mathbf{S}_{i,k+1}]^{\mathrm{T}}\end{aligned}$$

Hence, the square-root of the updated information matrix is given by

$$\boxed{\mathbf{S}_{y,k+1|k+1} = \mathbf{Tria}\big([\mathbf{S}_{y,k+1|k} \quad \mathbf{S}_{i,k+1}]\big)} \tag{1.28}$$

**Note**: When the local sensors employ the square-root information filtering algorithm, they are required to send the square-root information matrices to the fusion center (see Fig. 1.1). For a distributed sensor network with $n_s$ sensors, we may obtain $\mathbf{S}_{y,k+1|k+1}$ by augmenting the arguments on the right hand side of (1.28) with $n_s$ square-root information contribution matrices coming from $n_s$ sensors.

$$\mathbf{S}_{y,k+1|k+1} \quad = \quad \mathbf{Tria}\big([\mathbf{S}_{y,k+1|k} \;\; \mathbf{S}_{i,k+1}^{(1)} \ldots \mathbf{S}_{i,k+1}^{(n_s)}]\big). \tag{1.29}$$

TABLE I below summarizes the steps involved in the SCIF algorithm.

**TABLE 1.1**
**SCIF: Time Update**

1. Assume that at time $k$ that $(\hat{\mathbf{y}}_{k|k}, \mathbf{S}_{y,k|k})$ is known. Compute the square-root covariance matrix

$$\mathbf{S}_{k|k} \quad = \quad \mathbf{S}_{y,k|k}^{-\mathrm{T}} \tag{1.30}$$

2. Compute the state estimate

$$\hat{\mathbf{x}}_{k|k} \quad = \quad \mathbf{S}_{k|k}\mathbf{S}_{k|k}^{\mathrm{T}}\hat{\mathbf{y}}_{k|k} \tag{1.31}$$

3. Use the time-update of the SCKF to compute $\big(\hat{\mathbf{x}}_{k+1|k}, \mathbf{S}_{k+1|k}\big)$ from $\big(\hat{\mathbf{x}}_{k|k}, \mathbf{S}_{k|k}\big)$.
4. Compute the square-root of the predicted information matrix

$$\mathbf{S}_{y,k+1|k} \quad = \quad \mathbf{S}_{k+1|k}^{-\mathrm{T}} \tag{1.32}$$

5. Compute the predicted information vector

$$\hat{\mathbf{y}}_{k+1|k} \quad = \quad \mathbf{S}_{y,k+1|k}\mathbf{S}_{y,k+1|k}^{\mathrm{T}}\hat{\mathbf{x}}_{k+1|k} \tag{1.33}$$

**SCIF: Measurement Update**

1. Use the measurement-update of the SCKF to compute $\mathbf{T}_{11}$ and $\mathbf{T}_{21}$ from $\big(\hat{\mathbf{x}}_{k+1|k}, \mathbf{S}_{k+1|k}\big)$.
2. Compute the square-root of the information contribution matrix

$$\mathbf{S}_{i,k+1} \quad = \quad \mathbf{S}_{y,k+1|k}\mathbf{S}_{y,k+1|k}^{\mathrm{T}}\mathbf{T}_{21}\mathbf{T}_{11}^{\mathrm{T}}\bar{\mathbf{S}}_{R,k+1}, \tag{1.34}$$

where the inverse of the measurement noise covariance matrix

$$\bar{\mathbf{S}}_{R,k+1} \quad = \quad \mathbf{S}_{R,k+1}^{-\mathrm{T}}. \tag{1.35}$$

3. Compute the information contribution vector

$$\mathbf{i}_{k+1} = \mathbf{S}_{i,k+1}\bar{\mathbf{S}}_{R,k+1}\big(\mathbf{z}_{k+1} - \hat{\mathbf{z}}_{k+1|k}\big) + \mathbf{S}_{i,k+1}\mathbf{S}_{i,k+1}^{\mathrm{T}}\hat{\mathbf{x}}_{k+1|k} \quad (1.36)$$

4. Compute the updated information vector

$$\hat{\mathbf{y}}_{k+1|k+1} = \hat{\mathbf{y}}_{k+1|k} + \mathbf{i}_{k+1} \quad (1.37)$$

5. Compute the square-root of the updated information matrix

$$\mathbf{S}_{y,k+1|k+1} = \mathbf{Tria}\big([\mathbf{S}_{y,k+1|k} \;\; \mathbf{S}_{i,k+1}]\big). \quad (1.38)$$

## 1.4 Applications

### 1.4.1 Maneuvering target tracking in a distributed sensor network with feedback

Consider an air-traffic control scenario, where an aircraft executes maneuvering turn in a horizontal plane at a constant, but unknown turn rate $\Omega$. Fig. 1.4 shows a representative trajectory of the aircraft. The kinematics of the turning motion can be modeled by the following nonlinear process equation [3]:

$$\mathbf{x}_k = \begin{pmatrix} 1 & \frac{\sin\Omega T}{\Omega} & 0 & -\big(\frac{1-\cos\Omega T}{\Omega}\big) & 0 \\ 0 & \cos\Omega T & 0 & -\sin\Omega T & 0 \\ 0 & \frac{1-\cos\Omega T}{\Omega} & 1 & \frac{\sin\Omega T}{\Omega} & 0 \\ 0 & \sin\Omega T & 0 & \cos\Omega T & 0 \\ 0 & 0 & 0 & 0 & 1 \end{pmatrix} \mathbf{x}_{k-1} + \mathbf{v}_{k-1},$$

where the state of the aircraft $\mathbf{x} = [\mathbf{x}[1] \;\; \mathbf{x}[2] \;\; \mathbf{x}[3] \;\; \mathbf{x}[4] \;\; \mathbf{x}[5] = \Omega]^T$; $\mathbf{x}[1]$ and $\mathbf{x}[3]$ denote positions, and $\mathbf{x}[2]$ and $\mathbf{x}[4]$ denote velocities in the $x$ and $y$ directions, respectively; $T$ is the time-interval between two consecutive measurements; the process noise $\mathbf{v}_{k-1} \sim \mathcal{N}(\mathbf{0}, \mathbf{Q})$ with a nonsingular covariance $\mathbf{Q} = \mathrm{diag}[q_1\mathbf{M} \;\; q_1\mathbf{M} \;\; q_2 T]$, where

$$\mathbf{M} = \begin{pmatrix} \frac{T^3}{3} & \frac{T^2}{2} \\ \frac{T^2}{2} & T \end{pmatrix};$$

The scalar parameters $q_1$ and $q_2$ are related to process noise intensities. The radars were assumed to measure range and range-rate. For a radar located at $\mathbf{x}_s = \big[\mathbf{x}_s[1], \; \mathbf{x}_s[2]\big]^{\mathrm{T}}$, the measurement equation is given by

$$\mathbf{z}_k = \begin{pmatrix} \sqrt{(\mathbf{x}_k[1] - \mathbf{x}_s[1])^2 + (\mathbf{x}_k[3] - \mathbf{x}_s[2])^2} \\ \frac{(\mathbf{x}_k[1] - \mathbf{x}_s[1])\mathbf{x}_k[2] + (\mathbf{x}_k[3] - \mathbf{x}_s[2])\mathbf{x}_k[4]}{\sqrt{(\mathbf{x}_k[1] - \mathbf{x}_s[1])^2 + (\mathbf{x}_k[3] - \mathbf{x}_s[2])^2}} \end{pmatrix} + \mathbf{w}_k \quad (1.39)$$

where the measurement noise covariance $\mathbf{R}$ is given by

$$\mathbf{R} = \text{cov}[\mathbf{w}_k] \quad = \quad \text{diag}([\sigma_r^2 \ \sigma_{\dot{r}}^2]).$$

To make this nonlinear tracking problem highly difficult, the target trajectory was made up of four segments, in each of which $\Omega$ was set to be $5^\circ s^{-1}, -9^\circ s^{-1}, -3^\circ s^{-1}$ and $9^\circ s^{-1}$ for the duration of 0-40 s 40-70 s, 70-90 s and 90-100 s, respectively. We used the following parameters for simulation:

$$\begin{aligned} T &= 2\text{s} \\ q_1 &= 0.1\text{m}^2\text{s}^{-3} \\ q_2 &= 10^{-6}\text{s}^{-3} \\ \sigma_r &= 10\text{m} \\ \sigma_{\dot{r}} &= 10\text{m/s} \end{aligned}$$

The true initial state was assumed to be at

$$\mathbf{x}_0 \quad = \quad [0\text{m} \ 100\text{ms}^{-1} \ -400\text{m} \ 120\text{ms}^{-1} \ 2^o\text{s}^{-1}]^T,$$

The initial state estimate $\hat{\mathbf{x}}_{0/0}$ was chosen randomly from $\mathcal{N}(\mathbf{x}_0, \mathbf{P}_{0/0})$ in each run, where

$$\mathbf{P}_{0/0} \quad = \quad \text{diag}[100\text{m}^2 \ 25\text{m}^2\text{s}^{-2} \ 25\text{m}^2 \ 25\text{ms}^{-2} \ \ (1.7\text{mrads}^{-1})^2].$$

For a fair evaluation, we made a total of $N = 100$ independent Monte Carlo runs (The reader may refer to `http://haranarasaratnam.com/software.html` for a set of Matlab code used to generate the results). The radars were randomly placed in a square-shaped surveillance region with the opposite vertices at (-4000, -4000) and (4000, 4000). In this experiment, the number of radars, $n_s$, was varied from one to fifteen. We employed the following information filters for tracking the aircraft:

- Extended Information Filter(EIF)
- Cubature Information Filter (CIF)
- Square-root Cubature Information Filter (SCIF)

Note that the unscented information filter boils down to the CIF when the free parameter $\kappa$ is forced to take zero. For this reason, the unscented information filter was excluded from comparison.

For performance comparison, we computed the accumulative root mean-squared error (ARMSE) in position and velocity. The ARMSE yields a combined measure of the bias and variance of a filter estimate. We define the ARMSE in position

$$\text{ARMSE [pos]} \quad = \quad \sqrt{\frac{1}{N}\sum_{n=1}^{N}\frac{1}{K}\sum_{k=1}^{K}\left(\mathbf{x}_{k,n}[1] - \hat{\mathbf{x}}_{k|k,n}[1]\right)^2 + \left(\mathbf{x}_{k,n}[3] - \hat{\mathbf{x}}_{k|k,n}[3]\right)^2}$$

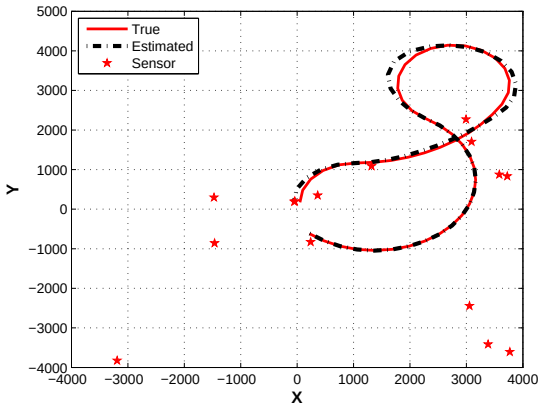


**FIGURE 1.4**
True aircraft trajectory– solid line, SCIF estimate– dotted line, ★ - Radar locations.

where $(\mathbf{x}_{k,n}[1],\ \mathbf{x}_{k,n}[3])$ and $(\hat{\mathbf{x}}_{k|k,n}[1],\ \hat{\mathbf{x}}_{k|k,n}[3])$ are the true and globally estimated positions at the $n$-th Monte Carlo run. Similarly to the ARMSE in position, we may also write formula of the ARMSE in velocity. To check the numerical robustness of an information filter, the filter divergence rate was introduced. The filter was declared to diverge when $\sqrt{\text{MSE [pos]}}$ of a specific Monte Carlo run exceeded 100m. Subsequently, those diverged runs were excluded from the final calculations of ARMSE [pos] and ARMSE [vel].

Figs. 1.5(a) and 1.5(b) show the ARMSE in position and velocity, respectively, for the SCIF and EIF. As expected, as the number of sensors $n_s$ increases, the ARMSEs in position and velocity decrease. However, the performance gain quickly diminishes; as $n_s > 5$, the performance gain seems to be trivial. Moreover, the SCIF consistently outperforms the EIF irrespective of $n_s$ although the performance deviation between the two reduces with $n_s$. The CIF is not included in Figs. 1.5(a) and 1.5(b) because its performance was almost identical to the SCIF.

Fig. 1.6 shows how many times each filter experienced divergence out of $N = 100$ independent Monte Carlo runs. As can be seen from Fig. 1.6, the EIF diverges the most. However, its divergence rate decreases as $n_s$ increases. The CIF diverges a few times especially when $n_s$ is less. The SCIF diverges a few times only when $n_s = 2$. Unlike the CIF, the SCIF does not diverge when $n_s = 3$ and 4. This observation indicates that the SCIF is superior to other filters in terms of numerical robustness. None of the filters diverged when $n_s \geq 7$.

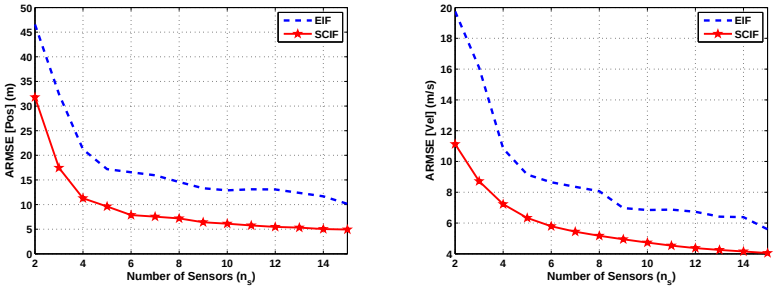


(a) Position Error (m) (b) Velocity Error (m/s)

**FIGURE 1.5**
Accumulative root mean-squared error in position and velocity

### 1.4.2 Speed and rotor position estimation of a two phase permanent magnet synchronous motor

In this subsection, we consider the speed and rotor position estimation of a two phase permanent magnet synchronous motor (PMSM). The kinematics of the PMSM can be expressed by the following process equation [8, 5]:

$$\begin{bmatrix} x_{1,k+1} \\ x_{2,k+1} \\ x_{3,k+1} \\ x_{4,k+1} \end{bmatrix} = \begin{bmatrix} x_{1,k} + T_s(-\frac{R}{L}x_{1,k} + \frac{\omega\lambda}{L}\sin x_{4,k} + \frac{1}{L}u_{a,k}) \\ x_{2,k} + T_s(-\frac{R}{L}x_{2,k} - \frac{\omega\lambda}{L}\cos x_{4,k} + \frac{1}{L}u_{b,k}) \\ x_{3,k} + T_s(-\frac{3\lambda}{2J}x_{1,k}\sin x_{4,k} + \frac{3\lambda}{2J}x_{2,k}\cos x_{4,k} - \frac{Fx_{3,k}}{J}) \\ x_{4,k} + T_s x_{3,k} \end{bmatrix}$$

The first two states are currents through the two windings, the third state is speed and the fourth state is rotor angular position. The objective is to estimate the rotor angular position and speed of PMSM using the two winding currents. The measurement equation is therefore given as follows:

$$\begin{bmatrix} y_{1,k} \\ y_{2,k} \end{bmatrix} = \begin{bmatrix} x_{1,k} \\ x_{2,k} \end{bmatrix}$$

For simulation, we chose the following parameters: R = 1.9Ω, $\lambda$=0.1, L = 0.003H, J = 0.00018, F = 0.001 and $T_s$ = 0.001 s. The process noise was assumed to zero mean Gaussian with the covariance as shown by

$$\mathbf{Q} = \begin{bmatrix} 11.11 & 0 & 0 & 0 \\ 0 & 11.11 & 0 & 0 \\ 0 & 0 & 0.25 & 0 \\ 0 & 0 & 0 & 1\times10^{-6} \end{bmatrix}$$

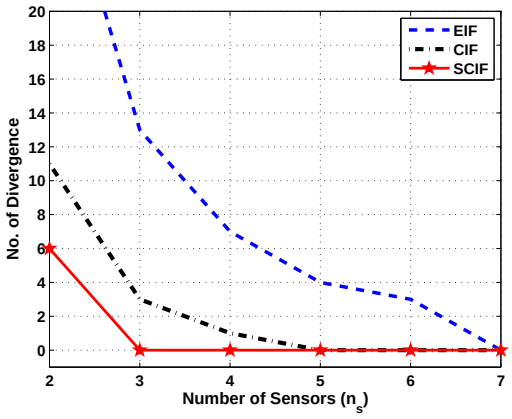


**FIGURE 1.6**
Number of divergence experienced in 100 independent Monte Carlo runs

The input excitation is given by

$$\begin{bmatrix} u_{a,k} \\ u_{b,k} \end{bmatrix} = \begin{bmatrix} \sin(0.002\pi k) \\ \cos(0.002\pi k) \end{bmatrix}.$$

Five current sensors were used to measure the output currents. They were assumed to provide measurements perturbed by zero mean Gaussian noise with covariances $\mathbf{R}_1 = 2.457 \times 10^{-5}$, $\mathbf{R}_2 = 6.097 \times 10^{-5}$, $\mathbf{R}_3 = 2.415 \times 10^{-5}$, $\mathbf{R}_4 = 0.1532 \times 10^{-5}$ and $\mathbf{R}_5 = 7.599 \times 10^{-5}$. The initial conditions of all the states were set to be $\mathbf{0}$ and the initial estimated state vector is selected from $\mathcal{N}\left(\begin{bmatrix} 0 & 0 & 0 & 0 \end{bmatrix}^T, 0.3162\mathbf{I}_4\right)$ for estimation. It was assumed that the first set of current sensors failed to provide measurements during the interval of 0.5 to 0.7 s and the outputs were assumed to be zero in this time interval. 50 Monte-Carlo runs were performed to evaluate the performance of the SCIF.

Figs. 1.7 and 1.8 show the results for the single and multi-sensor state estimation, respectively. It can be seen that the estimate of speed and rotor position using single sensor seems worse the multi-sensor estimate. The state estimation using the single sensor is not capable of providing a reliable estimate during the failure of a current sensor, whereas the multi-sensor based estimator is able to provide a reasonably accurate estimate. The estimated speed using single sensor takes 1.5s approximately to reach the actual speed, whereas in the multi-sensor case, the estimated speed quickly converges to the actual speed within 0.5s. The superior performance of the multi-sensor state estimation can be attributed to the fact that the final fused estimate is calculated by assigning more weights to 'more' accurate sensor measurements.

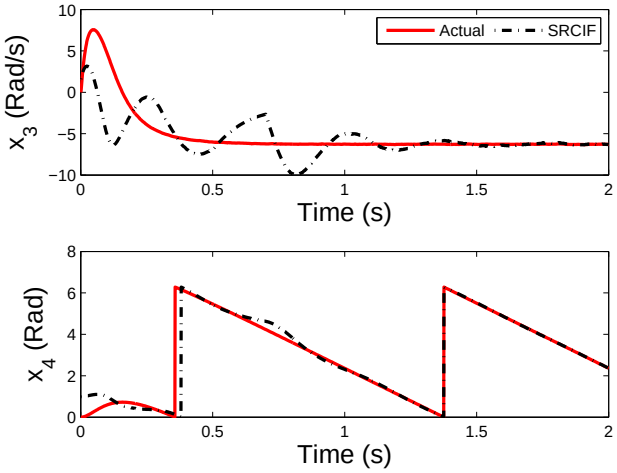


**FIGURE 1.7**
Actual and estimated speed and rotor positions using a single sensor

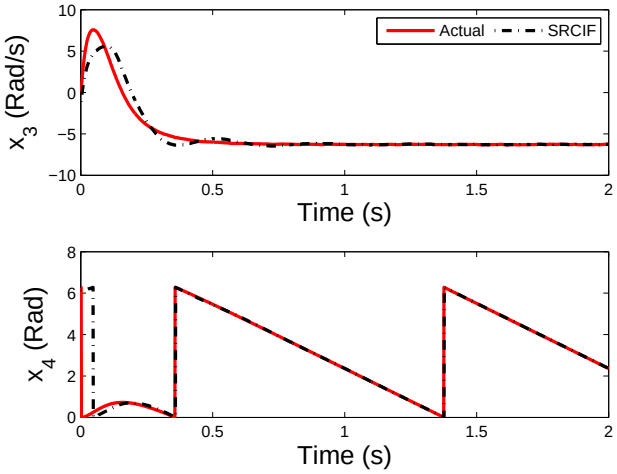


**FIGURE 1.8**
Actual and estimated speed and rotor positions using multi-sensors

## 1.5 Concluding Remarks

This chapter presented a numerically robust square-root cubature information filter (SCIF) algorithm for multi-sensor fusion in a nonlinear Gaussian environment. Because the SCIF propagates the square-root covariance matrices, it avoids to compute numerically sensitive matrix calculations. It was successfully demonstrated through computer experiments that the proposed SCIF algorithm is numerically accurate and robust. .

# Bibliography


[1] I. Arasaratnam, S. Haykin and T. R. Hurd, "Cubature Kalman Filtering for Continuous-Discrete Systems: Theory and Simulations," *IEEE Trans. Signal Processing*, 58(10), pp. 4977-4993, Oct 2010

[2] I. Arasaratnam and S. Haykin, "Cubature Kalman filters," *IEEE Trans. Automatic Cont.*, 54(6), pp. 1254-1269, June 2009

[3] Y. Bar Shalom, X. R. Li and T. Kirubarajan, *Estimation with Applications to Tracking and Navigation*, NY: Wiley & Sons, 2001

[4] Y. Bar-Shalom and X. R. Li, *Multitarget-Multisensor Tracking: Principles and Techniques*, YBS, Storrs, CT, 1995

[5] K. P. Bharani Chandra, D.-W Gu and I. Postlethwaite, "A square root Cubature information filter," IEEE Sensors Journal, vol. 13, no. 2, 2013, pp. 750-758.

[6] G. H. Golub and C. F. Van Loan, *Matrix Computations*, Baltimore:MD John Hopkins Univ. Press, 1996

[7] Y. Kim,, J. Lee, H. Do, B. Kim, T. Tanikawa, K. Ohba, G. Lee and J. Yun, "Unscented information filtering method for reducing multiple sensor registration error," *IEEE Int'l Conf. on Multisensor Fusion and Integration for Intelligent Systems*, pp. 326 331, 2008

[8] D. Simon, *Optimal Estimation: Kalman, $H_\infty$, and Nonlinear Approaches*, John Wiley & Sons, 2006.

[9] T. Vercauteren and X. Wang, "Decentralized Sigma-Point Information Filters for Target Tracking in Collaborative Sensor Networks," *IEEE Trans. Signal Pro.*, 53(8), pp. 2997-3009, 2005

[10] Y. Zhu, Z. You, J. Zhao, K. Zhang and X. Li, "The Optimality for the Distributed Kalman Filtering Fusion," *Automatica*, 37(9), pp. 1489-1493, 2001